Int J Adv Manuf Technol (2006) 31: 188–200
DOI 10.1007/s00170-005-0166-y

ORIGINAL ARTICLE

C. C. Ng · S. K. Ong · A. Y. C. Nee

Design and development of 3–DOF modular micro parallel kinematic manipulator

Received: 4 November 2004 / Accepted: 13 April 2005 / Published online: 16 March 2006

Abstract This paper presents the research and development of a 3–legged micro parallel kinematic manipulator (PKM) for positioning in micromachining and assembly operations. The structural characteristics associated with parallel manipulators are evaluated and the PKMs with translational and rotational movements are identified. Based on these identifications, a hybrid 3–UPU (universal joint–prismatic joint–universal joint) parallel manipulator is designed and fabricated. The principles of the operation and modelling of this micro PKM are largely similar to a normal-sized Stewart platform (SP). The overall size of the platform is contained within a space of 300 mm×300 mm×300 mm. A modular design methodology is introduced for the construction of this micro PKM. Calibration results of this hybrid 3–UPU PKM are discussed in this paper.

Keywords Stewart platform · Micro parallel kinematic manipulator · Workspace simulation · Modular design

1 Introduction

The increasing demand for high product quality, reduced product cost and shorter product development cycle results in a continuing need to achieve improvements in speed, versatility and accuracy in machining operations, especially high speed machining. Hence, the recent trends towards high speed machining have motivated research and development of new novel types of parallel kinematics machines [1].

C. C. Ng · A. Y. C. Nee (✉)
Singapore-MIT Alliance,
National University of Singapore,
9 Engineering Drive 1,
117576 Singapore, Singapore
e-mail: mpeneeyc@nus.edu.sg

S. K. Ong · A. Y. C. Nee
Mechanical Engineering Department,
Faculty of Engineering,
National University of Singapore,
9 Engineering Drive 1,
117576 Singapore, Singapore

A parallel manipulator is a closed-loop mechanism where a moving platform is connected to the base by at least two serial kinematics chains (legs). The conventional Stewart platform (SP) manipulator has six extensible legs and hence a very rigid kinematics structure [2]. The number of legs is usually equal to the number of degrees of freedom (DOF). Each leg is connected to a 3–DOF spherical joint at the platform and a 2–DOF universal joint at the base. Compared to serial kinematics manipulators, a SP has the desirable characteristics of high payload and rigidity, while the drawback is a much limited working envelope as well as more complex direct kinematics and control algorithms.

A conventional SP had earlier been developed at the National University of Singapore. This platform consists of six linear actuators independently driven by six stepper motors. It can perform translational movements and be implemented in precision engineering applications, such as fine motion control requiring multi-degrees freedom. The platform has been calibrated and found to be fairly accurate and repeatable. However, there are some limitations of this platform, namely, the complex direct kinematics solution, coupled problems of the position and orientation movements, as well as the expensive high precision spherical joints [3]. Further research is being performed to design and develop an improved SP.

A new trend in the development of parallel kinematics manipulators (PKM) is the reduction from six DOFs to three. The decrease of DOFs of the PKM has advantages in workspace and cost reduction. However, the 3–DOF PKM provides less rigidity and DOFs. To overcome these shortcomings, PKMs with fewer than six DOFs have been actively investigated. For example, Clavel [4] and Sternheim [5] reported a 4–DOF high speed robot called the Delta robot. Lee and Shah [6] analyzed a 3–DOF parallel manipulator. Although these two robots possess closed-form direct kinematics solutions, the Delta robot contains 12 spherical joints while Lee and Shah's manipulator contains three spherical joints. In addition, the position and orientation of Lee and Shah's manipulator are coupled. Some 3–DOF parallel manipulator architectures provide pure

relative rotation of the mobile platform about a fixed point and are used as pointing devices, wrists of manipulators and orienting devices [7, 8]. Recently, Tsai [9] introduced a novel 3–DOF translational platform that is made up of only revolute joints. It performs pure translational motion and has a closed-form solution for the direct and inverse kinematics.

Furthermore, the use of multi-axis robots is highly unjustified as several of the axes remain underutilized because of the redundancy in DOFs, which increases the complexity and cost. In addition, a purely 3–DOF translational or rotational motion would require the activation of all six legs, which means an increase in energy consumption [10]. Hence, in terms of cost and complexity, a 3–DOF 3–legged micro PKM is cost effective and the kinematics of the mechanism is further simplified for the purpose of control.

To increase the flexibility and functionality of the micro PKM developed in this research, the concept of modular design has been introduced. In recent years, modular robots have increasingly been proposed as a means to develop reconfigurable and self-repairable robotic systems [11]. To optimize the performance and self-repairability of a 3–legged 3–DOF PKM, the manipulation system needs to incorporate modularity and self-reconfiguration capabilities. Modular robots consisting of many autonomous units or modules can be reconfigured into a large number of designs. Ideally, the modules should be uniform and self-contained. The robot can change from one configuration to another manually or automatically. Hence, a modular manipulator can be reconfigured or modified to adapt to a new environment. The modules must interact with one another and co–operate to realize self-configuration. In addition, a modular micro PKM can have self-repairing capability by removing and replacing failed modules. Since self-reconfigurable modular robots can provide the functionality of many traditional mechanisms, they are especially suited for a variety of tasks, such as high speed machining [1] in the precision engineering industry.

2 Background

In this research, the objectives of the development of the micro PKM, i.e. micro parallel kinematic manipulator (MSP), are the minimization of the dimensions of the system and the portability of the system, e.g. portable on a CNC machine. With regards to the minimization of the dimensions of the MSP, the number of links of the platform is reduced from six to three. The DOF for a closed-loop PKM is examined using Grübler's formula:

$$F_e = \lambda(l - j - 1) + \sum_{i=1}^{j} f_i - I_d \tag{1}$$

where F_e is the effective DOF of the assembly or mechanism, λ is the DOF of the space in which the mechanism operates, l is the number of links, j is the number of joints, f_i is the DOF of the i–th joint and I_d is the idle or passive DOFs.

The number of joints is nine (six universal joints and three prismatic joints). The number of links is eight (two links for each actuator, the end effectors and the base). The sum of all the DOFs of the joints is 15. Hence, using Grübler's formula, the DOF of the micro PKM is computed as $F = 6(8 - 9 - 1) + 15 = 3$. Using a systematic enumeration methodology developed by Tsai [12], a comparison study of the configurations is performed to select a configuration that meets the requirement of the parallel kinematics system to be constructed in this research.

The research objective is to build a micro PKM with micron precision and that can withstand a load of up to 3 kg for the purpose of micromachining and assembly. Thus, high quality components need to be searched for to achieve the required accuracy. Even though a PKM is well known for its high accuracy, rigidity, speed as well as payload, the selection of the relevant parts needs to be carefully performed since the platform to be developed is used for micromachining, which requires a higher rigidity as compared to the previously developed platform. Therefore, based on the previously developed SP, various designs of PKMs are simulated on a micro scale using Matlab, such as the 6–legged SP, 3–legged PKM and 6–legged PUS SP, where PUS denotes a platform with links of prismatic joint, universal joint and spherical joint. The workspaces of these platforms are simulated and compared to select the most suitable design to achieve the research objectives.

In addition, the relationships between the workspace and the radii of the mobile platform and the fixed base are studied so that the workspace of the micro PKM is optimized. The maximum angle that the platform can be oriented is also deliberated based on the stroke of the actuators in order that it can be used as a reference for the selection of the actuators.

3 Simulation of various PKMs

3.1 Simulation models

Mathematical models of various kinds of PKMs that have currently been reported are investigated through performing simulations using Matlab. The workspaces of these PKMs are compared to identify a suitable PKM kinematics model for the present research. A 6–legged SP, 3–legged PKM and a PUS PKM are simulated using Matlab. The reasons for choosing the kinematics models of these manipulators are because they have a higher payload and are simple to control. All three models are shown in Fig. 1.

A series of simulations has been performed to determine the optimized workspace of the PKMs with suitable radii of the base and the platform, as well as passive spherical joints. In these simulations, certain parameters are kept as constant, such as the length of the link is set as 0.22 m with a stroke of 0.05 m. Besides, the tilting angle of the universal joint is set as ±45°.

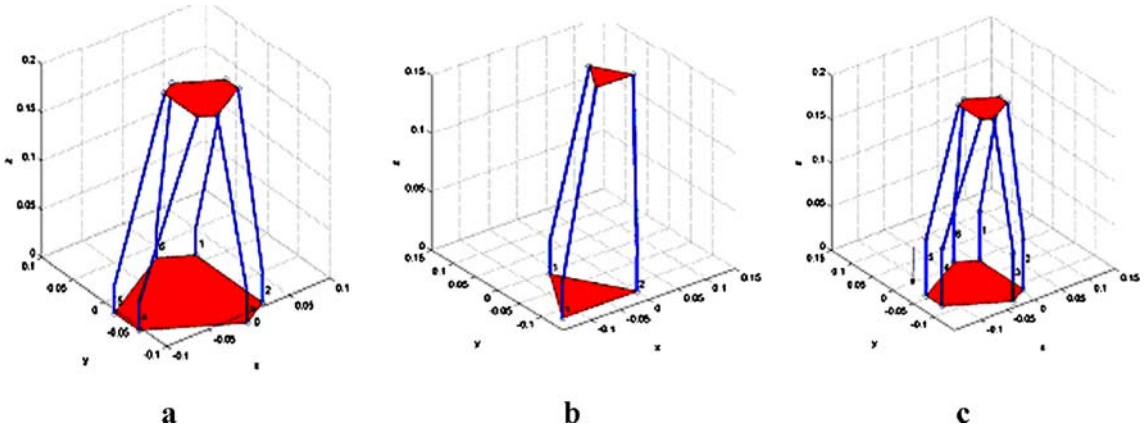

Fig. 1 **a** 6–legged micro Stewart platform, **b** 3–legged micro Stewart platform and **c** PSU micro Stewart platform

Using Matlab to simulate the motion of the each of the manipulators, the 3D position that the manipulator can reach is recorded (as shown in Fig. 2) and compared for all three PKMs. From Fig. 2, it can be observed that the workspace of the 6–legged parallel manipulator can reach a higher position. However, the volume of the workspace of the 3–legged parallel manipulator is larger.

3.2 Simulation results

In these simulations, the radius of the base of the PKM is set as 0.075 m. By varying the radius of the mobile platform of the PKM throughout these simulations, various workspaces are found, and the results are shown in Table 1 and Fig. 3. From these results, the workspace of the PKM is dependent on the radius of the mobile platform. Thus, the bigger the radius of the mobile platform, the larger is the workspace that can be achieved. However, a potential problem can be foreseen if the radius of the mobile platform is equal to the radius of the base. Singularity might happen at the point when the radii of mobile platform and the base are equal. The stiffness of the PKM might be reduced because all the joints are vertically upwards and the tension of the links between the mobile platform and the base may be reduced. In addition, the height of the PKM is also affected by the radius of the mobile platform. Since the length of the links is fixed, with a smaller mobile platform, the links can only be tilted to a certain angle to reduce the height of the platform.

In contrast to the relationships between the radius of the platform and the workspace, the workspace of the platform decreases while the radius of the base is increased, as shown in Table 2 and Fig. 4. In this simulation, the radius of the platform is set as 0.04 m.

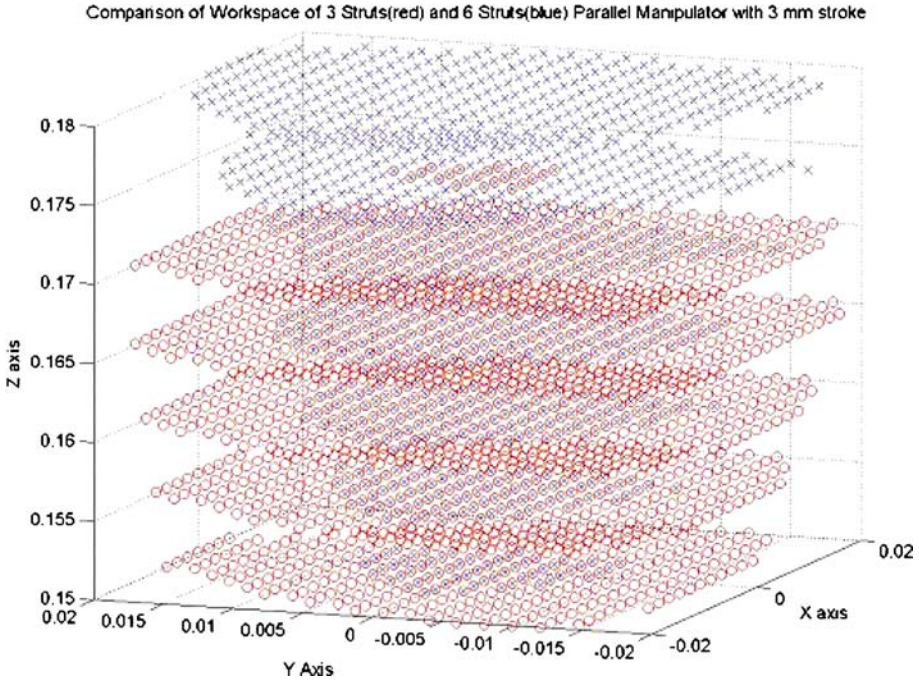

Fig. 2 Comparison of the workspace of 3–legged (*red circle*) and 6–legged (*blue cross*) parallel manipulators

Table 1 Workspaces of platform with varying platform radii

Radius of the micro SP, r	Workspace$\times 10^{-4}m^3$
0.035	3.0032
0.040	3.2810
0.050	5.7313
0.060	6.7163
0.070	9.9988
0.075	11.0000

Based on the analysis of the results of both simulations, when the difference between the size of the base and the platform becomes bigger, the workspace of the platform will become smaller. Thus, a ratio of 1:2 is suggested for the design of the radius of the mobile platform and the base.

3.3 Simulation result of relationships between the tilting angle of the spherical joints

In this investigation, the results of the workspace simulation are obtained by setting the base radius as 0.075 m and the platform radius as 0.03 m with varying passive spherical joint angles of 20° and 45°. From the results in Fig. 5, the workspace of the platform increased drastically when the tilting angle of the spherical joint varied from ±20° to ±45°. By installing a 45° spherical joint, the volume of the workspace can reach up to 0.0014 m^3 instead of 4.1263×10^{-4} m^3, i.e. a 3.4-fold increase, when a spherical joint of 20° is installed.

Simulation was also carried out to determine the maximum stroke that an actuator has made to achieve the largest orientation angle. Different actuators with various strokes are simulated to obtain the angles they could rotate. From the results, to achieve a 45° rotation for the mobile platform, the stroke of the actuators must be at least 50 mm.

From the study on the feasibility of the 3–legged MSP to achieve the objectives of this research, it is found that the DOF of the MSP is limited by the number of active joints. Thus, by having three prismatic actuators, there can only be three DOFs for the 3–legged MSP. According to Grübler's formula in Eq. 1, three prismatic actuators can perform three DOF movements. The stability of the legs, however, needs to be improved, such as by replacing the spherical joints with universal joints, or by installing certain constraining components, such as a rigid link connected to a spherical joint in the middle.

From literature studies of the parallel manipulators [10, 13], 3–DOF PKMs can be divided into three major types, namely, the planar parallel, spherical parallel and spatial parallel manipulators. In this paper, the study of spatial manipulators is focused, and they can perform either purely translational movements or rotational movements. However, the hybrid of both motions is feasible but the complexity will be increased. One of the attractive characteristics of 3–DOF PKMs is their flexibility and can adapt to the required function that they need to perform [14]. As an example, by coupling a 3–legged orientation mechanism PKM and a 3-legged translational mechanism parallel manipulator, a 6–DOF PKM can be achieved.

Hence, in this paper, the development of the purely translational PKM and rotational PKM is explored. However, the design and fabrication of a hybrid 3–UPU PKM is focused. A hybrid 3–UPU platform is a parallel manipulator that is installed with prismatic links, which are connected to the base and the platform with universal joints. Furthermore, a passive link is installed at the center of the platform using a spherical joint. One of the interesting

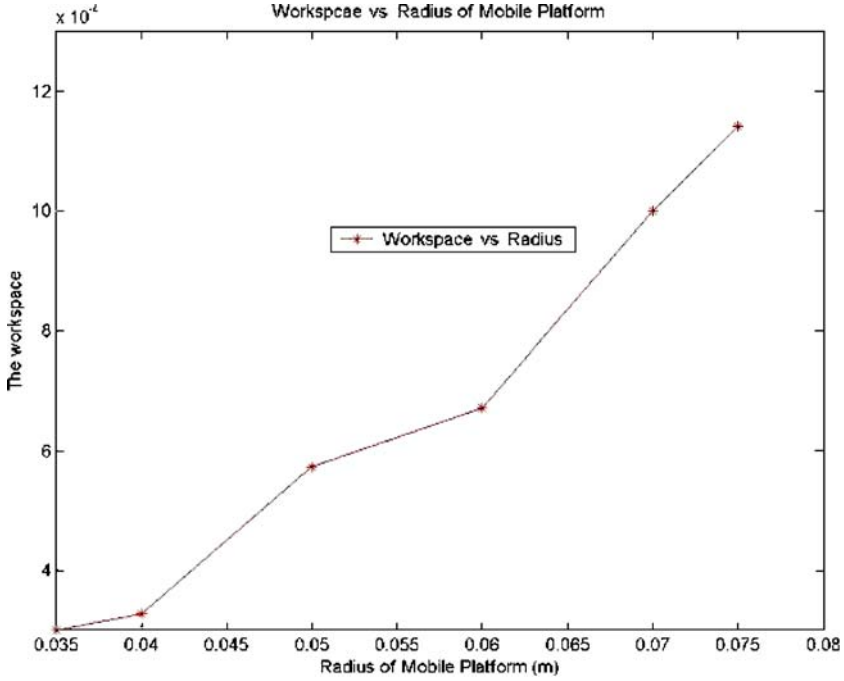

Fig. 3 Workspace versus radius of mobile platform

Table 2 Workspace of platform with varying base radii

The radius of the base, r	Workspace$\times 10^{-3}m^3$
0.075	0.4126
0.085	0.2760
0.095	0.1665
0.105	0.0826

features of this mechanism is that it has a hybrid movement of both the pure translational PKM and rotational PKM. It has a bigger workspace along the Z–axis while it can perform as a rotational mechanism. The specialty of this PKM is that it is able to play an interesting key role for manipulating some extra directions of movement and providing more flexibility if it is added to serial kinematics NC machines.

Hence, based on the results of the simulations, a 3–DOF MSP has been constructed with a 50 mm stroke actuator, a 125 mm diameter platform and a 250 mm diameter base, to achieve the requirements of the workspace and functions of the platform. A mathematical model of the MSP is developed in the next section. An optimization process has also been performed to finalize the workspace of the platform.

4 Mathematical model of hybrid 3–UPU PKM

To analyze the kinematics model of the parallel mechanism, two relative coordinate frames are assigned, as shown in Fig. 6. A static Cartesian coordinate frame $X_B Y_B Z_B$ is fixed at the center of the base while a mobile Cartesian coordinate frame $X_P Y_P Z_P$ is assigned to the center of the mobile platform. P_i, i=1,2,3 and B_i, i=1,2,3 are the joints that are located in the center of the base and the platform passive joints, respectively. A passive middle link L_m is installed at the middle of the platform. The purpose of the link is to constrain the kinematics of the platform to perform translation along the z–axis and rotational around the x– and y–axes.

Let r_B and r_P be the radii of the base and the platform passing though joints P_i and B_i (i=1,2,3), respectively. The position of B_i with reference to the fixed coordinate frame $X_B Y_B Z_B$ can be expressed as in Eq. 2.

$$B_1 = [r_B \ 0 \ 0]^T \quad B_2 = \left[-\frac{1}{2}r_B \quad \frac{\sqrt{3}}{2}r_B \quad 0\right]^T \tag{2}$$

$$B_3 = \left[-\frac{1}{2}r_B \quad -\frac{\sqrt{3}}{2}r_B \quad 0\right]^T$$

The positions of joints P_i, (i=1,2,3) are expressed with respect to the mobile frame $X_P Y_P Z_P$ as in Eq. 3.

$$P_1 = [r_P \ 0 \ 0]^T \quad P_2 = \left[-\frac{1}{2}r_P \quad \frac{\sqrt{3}}{2}r_P \quad 0\right]^T \tag{3}$$

$$P_3 = \left[-\frac{1}{2}r_P \quad -\frac{\sqrt{3}}{2}r_P \quad 0\right]^T$$

Since the MSP is proposed to be built within a space of 300 mm×300 mm×300 mm, the actuators with length of 216 mm are too long to be assembled directly to the base joints. Instead of assembling the actuators on top of the joints, the actuators are aligned parallel to the joints as shown in Fig. 11. Therefore, the calculation of the length of

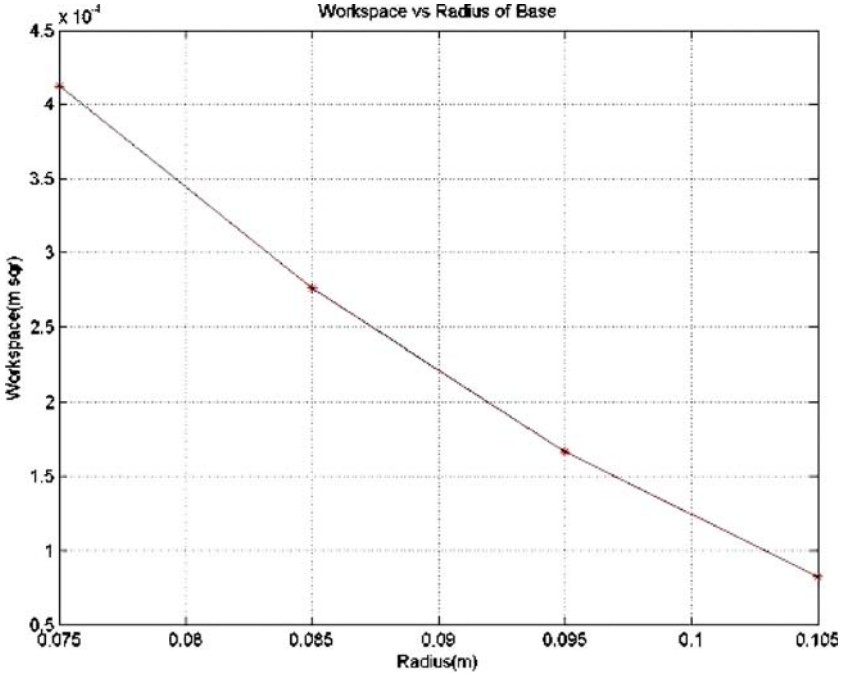

Fig. 4 Workspace versus radius of base

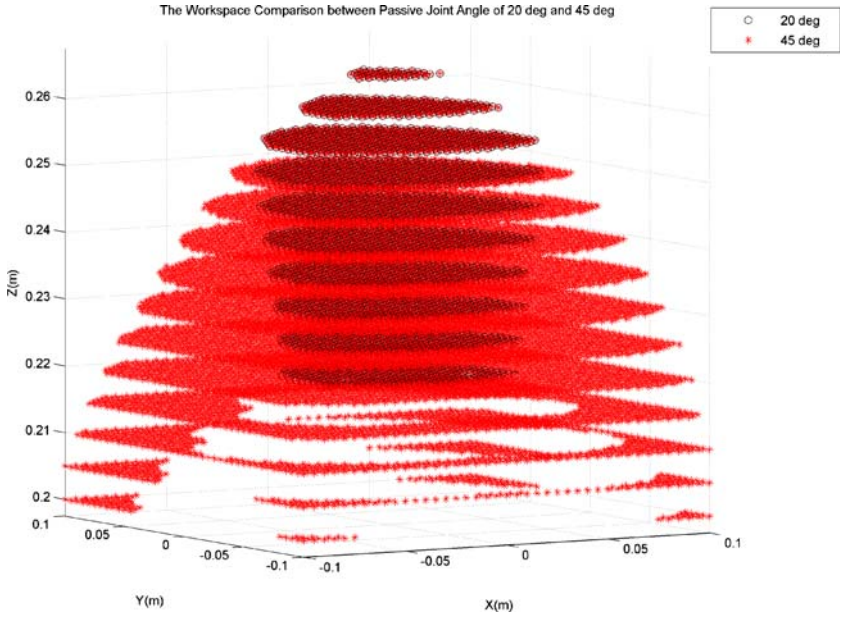

Fig. 5 Workspace comparison for passive joint angles of 20° (*circular point*) and 45° (*cross point*)

the link is not as direct as the inverse kinematics of a normal SP. As shown in Fig. 6, the length of the link can be calculated using Eq. 4.

$$\overrightarrow{l_i} = -\overrightarrow{B_i} + \overrightarrow{t} + \underline{R} \cdot \overrightarrow{P_i},\ i = 1 \ldots 3 \tag{4}$$

where l_i is the dotted link length, and $\overrightarrow{t}$ and R are the translation and orientation of P_i with respect to $[X_P\ Y_P\ Z_P]^T$. However, for this present hybrid PKM, extra calculation steps in Eqs. 5, 6, 7 and 8 are needed as shown in Fig. 7.

$$x^2 + a^2 = y^2 \tag{5}$$

$$\frac{k-x}{x} = \frac{z}{a} = \frac{L-y}{y} \Rightarrow y = \frac{xL}{k} \tag{6}$$

$$(5) \Rightarrow (6) \Rightarrow x = \sqrt{\frac{a^2}{\left(\frac{L^2}{k^2}\right) - 1}} \tag{7}$$

$$(7) \Rightarrow (6) \Rightarrow z = a \times \frac{k-x}{x} = \left(\frac{k - \sqrt{\frac{a^2}{\frac{L^2}{k^2}-1}}}{\sqrt{\frac{a^2}{\frac{L^2}{k^2}-1}}} \right) \times a \tag{8}$$

By determining the length of the dotted link, L_i using inverse kinematics, the length of Z can be determined using the similarity triangular theory as shown in Eq. 8. Hence the strokes of the links are found indirectly based on the manipulation of the platform. After analysing the stroke through inverse kinematics methods, the required rotational angle of the base joints and platform joints can be further affirmed through determining the angles of rotation as shown in Fig. 8.

The geometry matrix method of analysis was used since for parallel manipulators, it is often more convenient to employ the geometric method [13]. Generally, a vector loop equation is written for each limb, and the passive joint variables are eliminated among these equations as shown in Fig. 8.

Let X=α, Y=β, Z=σ and L_i+H=M_i, since L_i is known from the similarity triangle equation. Furthermore, Z_i (i=1,2,3) is known based on the coordination of each of the base joints, which are 0°, 120° and 240°. Besides, $B_i = \left[r_{xi}\, r_{yi}\, 0\right]^T$, i=1,2,3 is also known from Eq. 3. Based on inverse kinematics of the platform, one can determine

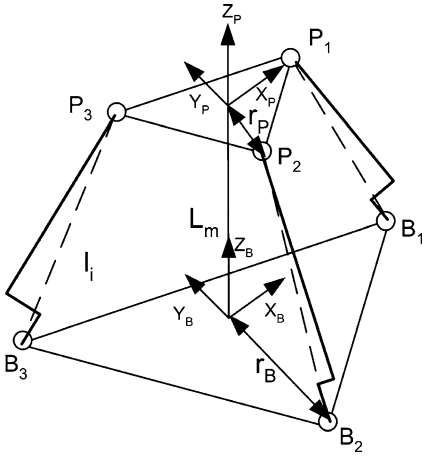

Fig. 6 Schematic diagram of the PKM

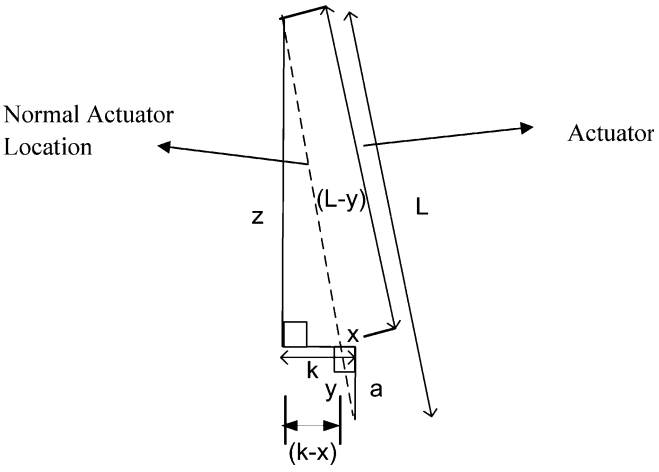

Fig. 7 Calculation of the actual stroke of the link

the point $\begin{bmatrix} P_{x_i} \\ P_{y_i} \\ P_{z_i} \end{bmatrix}$, i=1,2,3 from Eq. 4. Thus, for a known platform position, one can calculate the rotation angles, X_i and Y_i based on the known actuator stroke length using Eq. 9.

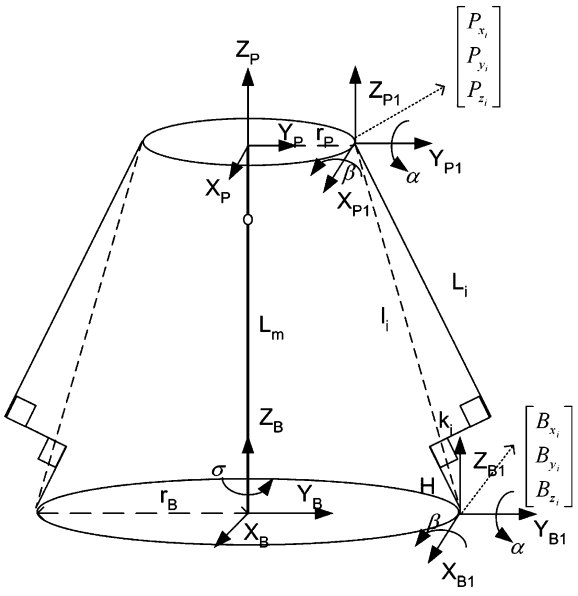

Fig. 8 Geometry method diagram

$$\therefore R_z \times R_{xy} \times \begin{bmatrix} 0 \\ k_i \\ M_i \end{bmatrix} + \begin{bmatrix} r_{xi} \\ r_{yi} \\ 0 \end{bmatrix} = \begin{bmatrix} P_{x_i} \\ P_{y_i} \\ P_{z_i} \end{bmatrix} \tag{9}$$

$$\begin{bmatrix} \cos Z_i & -\sin Z_i & 0 \\ \sin Z_i & \cos Z_i & 0 \\ 0 & 0 & 1 \end{bmatrix} \times \begin{bmatrix} \cos Y_i & \sin Y_i \sin X_i & \sin Y_i \cos X_i \\ 0 & \cos X_i & -\sin X_i \\ -\sin Y_i & \cos Y_i \sin X_i & \cos Y_i \cos X_i \end{bmatrix} \times \begin{bmatrix} 0 \\ k_i \\ M_i \end{bmatrix} + \begin{bmatrix} r_{x_i} \\ r_{y_i} \\ 0 \end{bmatrix} = \begin{bmatrix} P_{x_i} \\ P_{y_i} \\ P_{z_i} \end{bmatrix}$$
$$\Rightarrow \begin{bmatrix} (-\cos Y_i \sin Z_i + \sin Y_i \sin X_i \cos Z_i)k_i + \sin Y_i \cos X_i \times M_i + r_{x_i} \\ \cos X_i \cos Z_i \times K_i - \sin X_i \times M_i + r_{y_i} \\ (\sin Y_i \sin Z_i + \cos Y_i \sin X_i \cos Z_i)K_i + \cos Y_i \cos X_i \times M_i \end{bmatrix} = \begin{bmatrix} P_{x_i} \\ P_{y_i} \\ P_{z_i} \end{bmatrix} \tag{10}$$

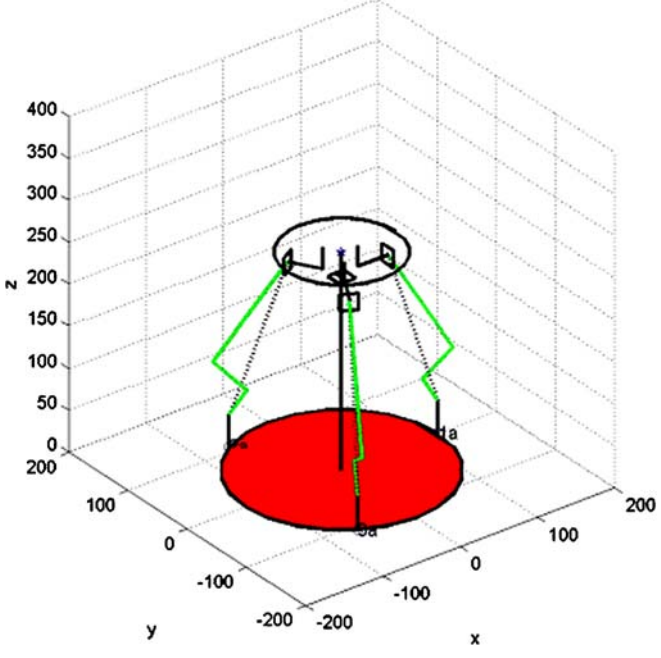

Fig. 9 Modified SP with a passive prismatic middle link

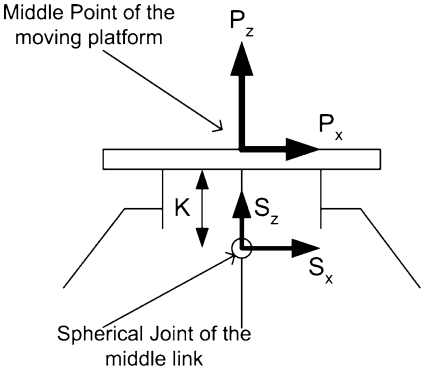

Fig. 10 Relationship between the point P and the spherical joint S

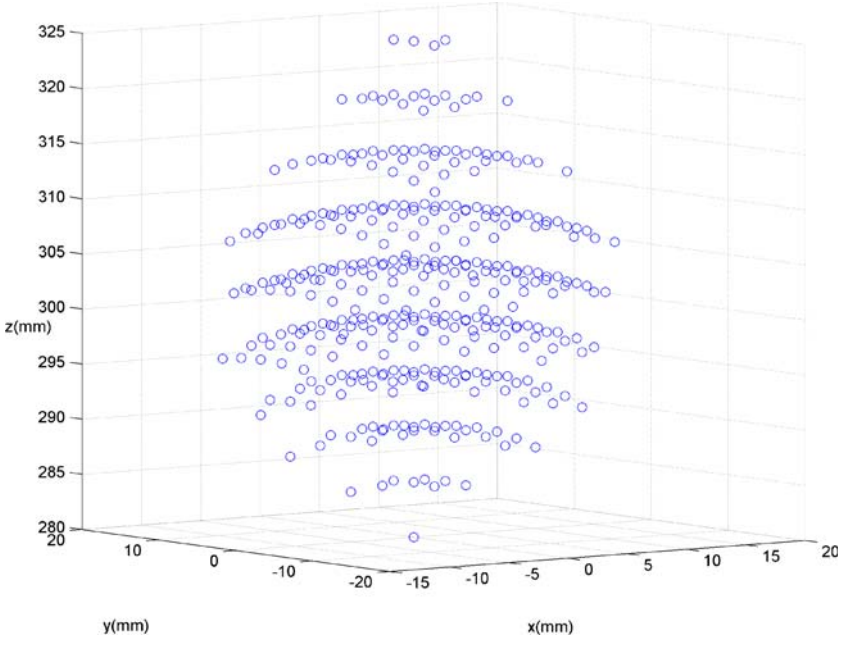

Fig. 11 Workspace of the surface point of the hybrid PKM

Hence,

$$X_i = 2 \times \tan^{-1}\left[\frac{2M_i \pm \sqrt{(2M_i)^2 - 4\left(r_{y_i} - P_{y_i} - \cos Z_i \times K_i\right)\left(\cos Z_i \times K_i + r_{y_i} - P_{y_i}\right)}}{2\left(r_{y_i} - P_{y_i} - \cos Z_i \times K_i\right)}\right] \tag{11}$$

$$Y_i = 2 \times \tan^{-1}$$

$$\left[\frac{2\sin Z_i \times K_i \pm \sqrt{(2\sin Z_i \times K_i)^2 - 4(P_{z_i} + \sin X_i \cos Z_i \times K_i + \cos X_i \times M_i)(P_{z_i} - \sin X_i \cos Z_i \times K_i - \cos X_i \times M_i)}}{2(P_{z_i} + \sin X_i \cos Z_i \times K_i + \cos X_i \times M_i)}\right] \tag{12}$$

Fig. 12 The PI M–235.5DG actuator (http://www.pi.ws), Huco Miniature Acetal Fork Type universal joint (http://www.huco.com) and Hephaist Seiko spherical joint (http://www.hephaist.co.jp/e/pro/ball.html)

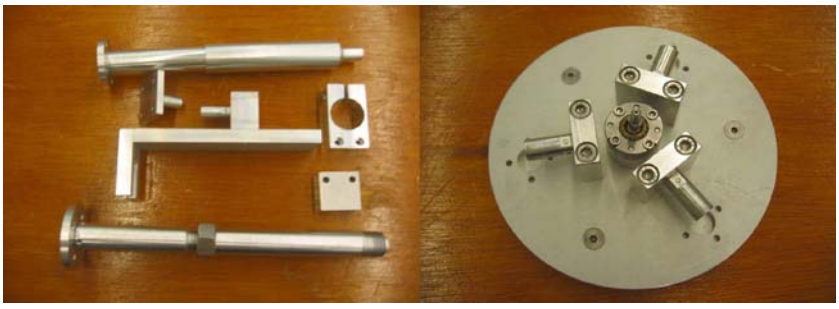

Fig. 13 The connectors, links and the mobile platform

Through Eqs. 11 and 12, the solutions for the rotation angle X_i, Y_i where i=1,2,3 can be found. Hence, through determining the rotation angle of each universal joint of the links, the stroke of the actuators can be determined. The known rotation angle is also used as a geometry constraint to determine the workspace of the platform. After the determination of the stroke and angle of rotation of all the universal joints of the actuators, a simulated hybrid 3–UPU PKM can be plotted using Matlab as shown in Fig. 9. A passive middle link is installed and attached via a spherical joint to the platform as shown in Fig. 10. The passive middle link acts as a constraint for the extra DOF of the platform. The inverse and forward kinematics algorithms of this hybrid PKM are implemented using Matlab, and the movement of the platform is simulated to verify the mobility of the platform.

5 Optimization method and analysis of workspace

Based on the inverse and forward kinematics algorithms of the platform, and due to the fact that all legs are equal and the distance between the joints at the base and platform are equilateral, the workspace of the hybrid 3–UPU platform depends on three geometric parameters, namely, (1) the stroke of the prismatic link, L_i, (2) the limitation of the universal joint angle of the base and platform, which is 45° and (3) the distances K between the spherical joint of the middle link to the middle point of the moving platform as shown in Fig. 10.

The stroke L_i of the actuator is the travel range of each prismatic link, which is 50 mm. As shown in Fig. 11, the workspace describes the manipulation of point *P*, which is at the middle of the mobile platform, with respect to the middle point *B* of the base, as shown in Fig. 10. For each orientation of the platform, the middle point *P* is rotated with respect to point *S* at the center of the spherical joint, which is located at the middle link of the platform as shown in Fig. 10.

During the optimization process, each position of the point *P* at the mobile platform is verified with its geometry constraints for every manipulation of the platform. The lengths of the legs are determined using inverse kinematics, i.e. Eq. 8. Next, the lengths of the legs are checked to determine if they are within the allowable interval $L_{min}<L_i<L_{max}$ and the interference of the legs is also checked. In addition, for rotation movements of the platform, the joint angles are determined and verified. After all the geometry constraints have been verified, the verified Cartesian coordinates of point *P* are recorded in the workspace database.

The workspace optimization programme is implemented using Matlab. The workspace data points collected using the optimization programme are plotted using Matlab as shown in Fig. 11. Figure 11 shows the workspace of the optimal constrained configuration. The points represent the position that can be achieved by point *P* of the mobile platform. The workspace of point *P* describes a portion of a sphere with its center at point *S* and a radius *K*. The workspace volume of point *P* increases gradually during the incremental motion of point *P* along the z–axis. The workspace volume increases to its maximum when the platform is located at z=310 mm. Overall, the workspace forms a diamond shape. The volume of the workspace is

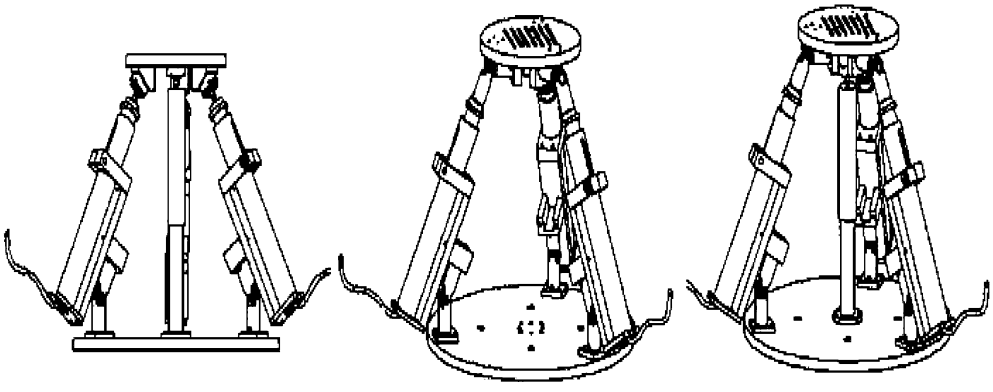

Fig. 14 Parallel manipulator systems fabricated using the same modular components

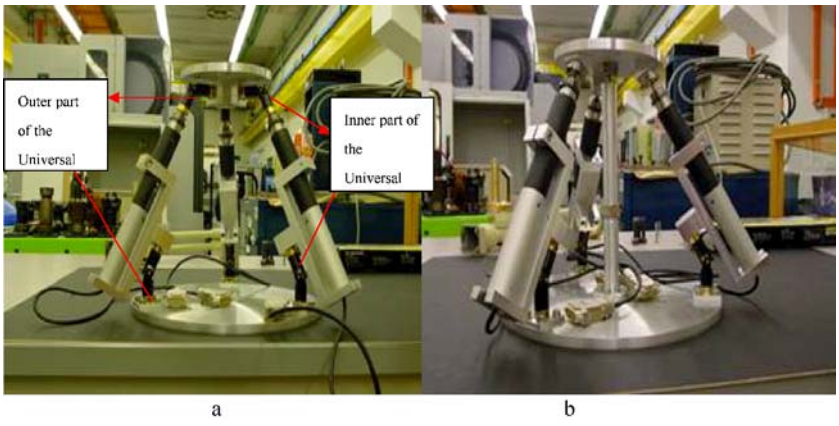

Fig. 15 **a** Pure translational platform, **b** pure rotational platform

93,875 mm^3, which is relatively small as compared with other modular PKM configurations. However, the objective of this hybrid micro PKM is for fine machining movements along the z–axis as well as rotational movements around the x– and y–axes. Hence, the simulated workspace shows that the platform is constrained from over traveling. Although this system has a limited Cartesian workspace, in terms of angular workspace, it can rotate up to 32° around the x–axis and 28.2° around the y–axis when z=310 mm. Furthermore, the platform can travel 450 mm along the z–axis. From the results of the workspace analysis, the workspace is affected significantly by the limitation of the stroke of the actuators and the imposed angle of the universal joints.

6 Design of the micro parallel manipulator

A set of design criteria that has been formulated based on the literatures review of PKMs and the results of the workspace analysis is applied in the fabrication and design of the hybrid 3–UPU PKM. To shorten the development cycle [2], the modular design methodology is employed in the prototype development.

Fig. 16 Hybrid 3–UPU PKM

Basically, a modular parallel robot consists of a set of independently designed modules, such as actuators, passive joints, rigid links (connectors), mobile platforms and end-effectors that can be rapidly assembled into various configurations with different kinematics characteristics and dynamic behaviors. There are many configurations of a modular platform. Hence, the development of a methodology for design and dimensional synthesis of a parallel robot system for a specific task is a basic and important requirement [15]. Based on the research reported by Dash et al. [15], a modular parallel robot may have an unlimited number of configurations depending on the inventory of the modules. Principally, the modules for assembly into a modular micro PKM can be divided into two groups:

1. Fixed dimension modules

Fig. 17 Calibration of micro PKM using CMM

This group includes actuator modules, passive joint modules (rotary, pivot and spherical joints) and end-effector joints, such as the PI M–235.5DG actuators, Hephaist spherical joints and miniature acetal fork type universal joints (Fig. 12).

2. Variable-dimension modules
   This group provides the end users with the ability to rapidly fine-tune the kinematic and dynamic performance of the manipulators, such as rigid links, joint connectors and platform modules, which can be rapidly assembled into various layouts with different kinematic and dynamic characteristics.

As shown in Fig. 13, a set of links and a mobile platform have been designed and fabricated. Through a combination of these modules, different configurations of modular PKMs can be assembled based on the functionality and purpose of the required manipulator. Based on the modular design concept, three PKMs are configured virtually using Solidworks and the same modular components as shown in Fig. 14. In Fig. 14, platforms with only rotational movements, translational movements, as well as a hybrid UPU platform can be assembled by interchanging the spherical and the universal joints or adding extra rigid links.

7 Prototype development

As stated earlier, as the actuators and joint modules are interchangeable, and the connectors can be fabricated in a very short period due to the simple design as shown in Fig. 13, this modular design approach has helped to reduce the complexity of design problems to a manageable level. Therefore, based on these concepts, three PKM prototypes have been developed and assembled to compare their characteristics and functions in an actual working environment. Two interchangeable prototypes of 3–DOF PKMs are assembled as shown in Fig. 15, which shows a pure translational PKM and a pure rotational PKM.

To maintain a high rigidity of the platforms, the DOFs of these systems can be constrained through the installation of extra joints or the reduction of the DOF of the joints. For the 4–legged platform in Fig. 15a, a fixed rigid link with a spherical joint is installed in the middle of the platform so that the motion of the platform is limited to angular rotation only. Thus, it can perform pure rotational movements. For the system in Fig. 15b, the spherical joints of the platform have been replaced with universal joints.Hence, this platform is limited to translational movements through the axes of the universal joints. Another 3–DOF PKM is configured

Table 3 Calibration result of the micro SP

Theoretical Position and Orientation			Actual Position and Orientation			Position and Orientation Error		
Rotation X°	Rotation Y°	Position Z (mm)	Z-10.426 (mm)	Actual X°	Actual Y°	Z error (mm)	Angle X error°	Angle Y error °
0	0	279	278.8502	-0.0452256	-0.365286	-0.1498	0.045225568	0.365286
0	0	304	304.157	-0.0397824	-0.372792	0.157	0.039782411	0.372792
0	0	279	278.887	-0.0545076	-0.367864	-0.113	0.054507585	0.367864
0	0	304	304.1532	-0.0385792	-0.377662	0.1532	0.038579187	0.377662
0	0	279	278.8512	-0.0448245	-0.369812	-0.1488	0.044824494	0.369812
0	0	328	328.4152	-0.0470018	-0.395424	0.4152	0.047001757	0.395424
0	0	279	278.7997	-0.0487779	-0.372276	-0.2003	0.048777945	0.372276
0	0	314	314.2583	-0.0551378	-0.382016	0.2583	0.055137845	0.382016
5	0	314	314.4069	4.9566289	-0.478564	0.4069	0.043371086	0.478564
10	0	314	314.1093	10.005325	-0.708506	0.1093	-0.0053253	0.708506
15	0	314	313.1804	15.051127	-1.091752	-0.8196	-0.05112695	1.091752
20	0	310	309.0273	20.087883	-1.563315	-0.9727	-0.08788319	1.563315
-5	0	310	309.7469	-5.0196374	0.3754471	-0.2531	0.019637435	-0.37545
-10	0	310	309.1461	-10.025349	-0.128134	-0.8539	-0.02535	-0.12813
-15	0	310	307.8201	-15.026953	0.8498897	-2.1799	-0.02695	0.84989
-20	0	310	307.3897	-19.908848	2.1461184	-2.6103	0.091152	2.146118
0	5	310	309.9521	0.3101281	4.5267511	-0.0479	0.310128	-0.47325
0	10	310	309.5268	0.5645316	9.5351477	-0.4732	0.564532	-0.46485
0	15	310	309.1953	0.8663929	14.535792	-0.8047	0.866393	-0.46421
0	20	310	306.751	1.1710863	19.495447	-3.249	1.171086	-0.50455
0	-5	310	309.8145	-0.0267188	-5.48063	-0.1855	-0.02672	-0..48063
0	-10	310	310.0537	-0.0847028	-10.51162	0.0537	-0.0847	-0.51162
0	-15	310	310.9903	-0.25665	-15.54496	0.9903	-0.25665	-0.54496
5	5	310	309.9001	5.1334433	4.4381289	-0.0999	0.133443	-0.56187
10	10	310	310.2003	9.8857264	9.6356161	0.2003	-0.11427	-0.36438
-5	-5	310	310.3308	-5.0607633	-5.386758	0.3308	-0.06076	-0.38676
-10	-10	310	310.0731	-10.365204	-10.03466	0.0731	-0.3652	-0.03466
-15	-15	310	308.0145	-15.678278	-14.33112	-1.9855	-0.67828	0.668877

= Maximum Error

as shown in Fig. 16. It is a hybrid 3–DOF platform that consists of translation movements along the z–axis and rotation movements around the x– and y–axes.

Nevertheless, there are advantages of a 3–DOF PKM. The control of a 3–DOF PKM is less complex and the rigidity can be increased. Furthermore, due to the introduction of the modular design concept through fabricating interchangeable parts, the 3–DOF PKM can be easily modified from a translational platform to a rotational platform. An extra link or active joints can be introduced in future to increase the DOF of the micro PKM.

Calibrations and various tests have been performed on the modular PKMs. Architectural singularities [16] have been detected during the calibration of the pure translational PKM while it is in the static position. It is found that in a static position, extra DOFs are introduced as some geometry conditions are not met, such as all the revolute pair axes at the ends of the links do not converge towards a single point, and each link has two intermediate resolute pair axes that are not parallel to one another and perpendicular to the straight line through the centre of the universal joint [17]. Hence, a careful assembly of the modular units of the platform satisfying certain geometry conditions is needed to attain a controllable pure translational motion.

For the rotational PKM, the platform is able to perform 3–DOF rotational movements in the roll, pitch and yaw directions. Since all the links are composed of 2–DOF universal joints, prismatic links and 3–DOF spherical joints, by installing a fixed link with a spherical joint at the centre of the platform, the motion of the platform is limited to purely rotational movements around a fixed point. The major disadvantage of this type of configuration is that the platform cannot perform z–axis movements, which is a crucial requirement for micromachining. The over-constrained design of this platform with a fixed middle link causes a high risk of damage to the platform when it is manipulated outside the defined workspace.

Hence, a hybrid PKM has been assembled by installing a passive prismatic link at the centre of the pure translational platform as shown in Fig. 16, and the singularity problem is solved. By installing a passive prismatic link in the middle of the platform and attached to the platform by a spherical joint, the extra DOF caused by the universal joints of the links is constrained. Thus, the hybrid PKM is able to perform movements along the z–axis and rotation about the x– and y–axes. Among the three PKMs' architectures that have been configured, the hybrid platform is further elaborated as it can be coupled with the present normal-sized SP to perform as a micro manipulator for a tool holder to perform machining operations on a workpiece that is fixtured on the SP. Calibration of the hybrid PKM was performed and the results showed that the accuracy of the movement is 0.5 mm and 0.02°.

8 Error calibration with CMM

After the development of the simulation and interfacing programmes, error calibration was performed using a CMM machine. The accuracy and repeatability of the platform was determined to be 100 micron. The set-up of the micro PKM on the CMM machine is shown in Fig. 17.

The calibration was performed by manipulating the platform to the theoretical positions and orientations using the visual C++ interface. Next, the data of the coordinates from the surface of the platform were collected to determine the actual surface plane of the platform. Using the CMM machine, the measurement variations between the actual angle and position and the theoretical angle and position were compared. The result of the calibration is shown in Table 3.

From Fig. 18, the maximum error of the roll angle is 1.171°, the maximum error of the pitch angle is 2.1461° and the maximum error of the z–axis displacement is −3.249 mm. At least two errors occurred in the same data set when the platform was translating and rotating simultaneously within the allowable maximum rotation angles. However, when the platform was performing purely translation movements, the error of the displacement was within ±0.42 mm.

The variations of the angular rotation and the translation movement of the z–axis are acceptable. The overall average errors of the angular rotation and translation are 0.063942° for the roll rotation, 0.186244° for the pitch rotation and 0.42854 mm for the z–axis movement. From

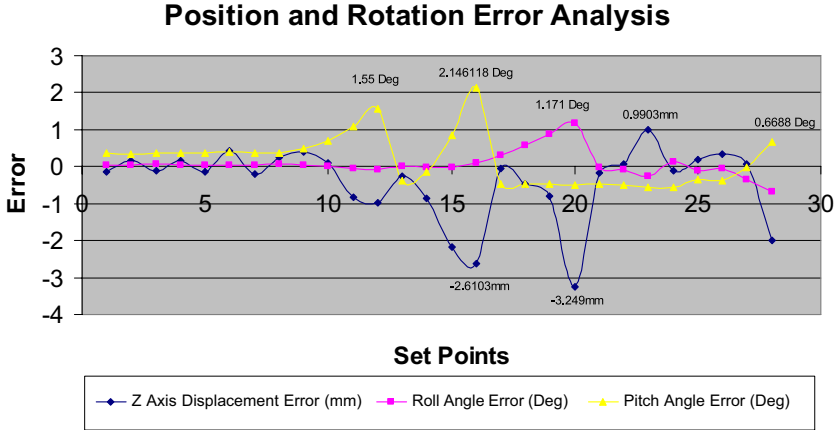

Fig. 18 Displacement and rotational error analysis

the calibration results, the errors of the rotational angle and position increase when the platform has reached the maximum rotational angle, which is the boundary of the calculated workspace.

9 Conclusions

This paper addresses the kinematics analysis of the hybrid PKM that has been designed and developed in this research to perform translation along the z–axis and rotation about the x– and y–axes. Modular configurations of the various PKMs are successfully assembled using the same modular units. An algorithm for the optimal design of the hybrid PKM has been presented. In particular, the proposed formulation represents an integration of the relevant aspects of the dimensional design of parallel manipulators in a multi-objective optimization design using workspace characteristics. A 3–DOF PKM has been constructed with which inverse kinematics can be solved analytically. The developed inverse kinematics algorithm of the PKMs can be used for similar modular platform configurations through using different constraint settings. This algorithm has been successfully implemented to control the hybrid PKM. The hybrid micro PKM that has been developed is calibrated based on the simulated workspace. The average errors are within 0.2° and 0.5 mm. In conclusion, the platform is able to travel to the required position and orientation smoothly and accurately for the precision engineering industry.

References

1. Joshi SA, Tsai LW (2003) The kinematics of a class of 3–DOF, 4–legged parallel manipulators. Trans ASME 125:52–60
2. Yang G, Chen IM, Chen WH, Yeo SH (2003) Design and analysis of a 3–RPRS modular parallel manipulator for rapid deployment. In: Proceedings of the IEEE/ASME International Conference on Advanced Intelligent Mechatronics, Kobe, Japan, pp 1250–1255
3. Tsai LW, Walsh GC, Stamper RE (1996) Kinematics of a novel three DOF translational platform. In: Proceedings of the 1996 IEEE International Conference on Robotics and Automation, Minneapolis, MN, 22–28 April 1996, pp 3446–3451
4. Clavel R (1988) DELTA, a fast robot with parallel geometry. In: Proceedings of the 18th International Symposium on Industrial Robots, Lausanne, Switzerland, 26–28 April 1988, pp 91–100
5. Sternheim F (1987) Computation of the direct and inverse kinematics model of the Delta 4 parallel robot. Robotersysteme 3:199–203
6. Lee K, Shah DK (1987) Kinematic analysis of a three degrees of freedom in-parallel actuated manipulator. In: Proceedings of the IEEE International Conference On Robotics and Automation, Raleigh, NC, 31 March–3 April 1987, pp 345–350
7. Asada H, Cro Granito JA (1985) Kinematic and static characterization of wrist joints and their optimal design. In: Proceedings of IEEE International Conference on Robotics and Automation, St. Louis, MO, 25–28 March1985, pp 91–100
8. Gosselin C, Hamel J (1994) The agile eye: agile performance three–degree–of freedom camera–orienting device. In: Proceedings of the IEEE International Conference on Robotics and Automation, San Diego, CA, 8–13 May 1994, pp 781–786
9. Tsai LW, Walsh GC, Stamper R (1996) Kinematics of a novel three DOF translational platform. In: Proceedings of the 1996 IEEE International Conference on Robotics and Automation, Minneapolis, MN, 22–28 April 1996, pp 3446–3451
10. Badescu M, Mavroidis C, Morman J (2002) Workspace optimization of orientational 3–legged UPS parallel platforms. In: Proceedings of the 2002 ASME International Design Engineering Technical Conferences and the Computers and Information in Engineering Conference (DETC/CIE), Montreal, Canada, 29 September–2 October 2002, DETC2002/MECH–34366, pp 1–7
11. Mckee G, chenker P (1999) Sensor fusion and decentralized control in robotic systems II. SPIE Proc Ser 3839:270–278
12. Tsai LW (1999) Robot analysis: the mechanics of serial and parallel manipulators. Wiley, New York, pp 116–164
13. Tsai LW (2000) Mechanism design: enumeration of kinematic structures according to function, CRC Press, Boca Raton, FL, ISBN 0–8493–0901–8
14. Tsai LW, Joshi S (2002) Kinematic analysis of 3–DOF position mechanisms for use in hybrid kinematic machines. J Mech Des 124:245–253
15. Dash AK, Chen IM, Yeo SH, Yang GL (2003) Task-based configuration design for 3–legged modular parallel robots using simplex methods. In: Proceedings of the 2003 IEEE International Symposium on Computational Intelligence in Robotics and Automation, Kobe, Japan, 16–20 July 2003, pp 998–1003
16. Ma O, Angeles J (1991) Architecture singularities of platform manipulators. In: Proceedings of the 1991 IEEE International Conference on Robotics and Automation, Sacramento, CA, 9–11 April 1991, pp 1542–1547
17. Gregorio RD (2001) Statics and singularity loci of the 3–UPU wrist. In: Proceedings of the 2001 IEEE/ASME International Conference on Advanced Intelligent Mechatronics, Como, Italy, 8–12 July 2001, pp 470–475